JOURNAL OF CATALYSIS **178,** 687–700 (1998)
ARTICLE NO. CA982203

Chromium Oxide/Alumina Catalysts in Oxidative Dehydrogenation of Isobutane

B. Grzybowska,*[,1] J. Słoczyński,* R. Grabowski,* K. Wcisło,* A. Kozłowska,* J. Stoch,* and J. Zieliński†

*Institute of Catalysis and Surface Chemistry, Polish Academy of Sciences, Niezapominajek, 30-239 Kraków, Poland; and † Institute of Physical Chemistry, Polish Academy of Sciences, 01-224 Warsaw, Kasprzaka 44/52, Poland

Received April 6, 1998; revised June 9, 1998; accepted June 9, 1998

The chromium oxide-alumina catalysts of the Cr loading varying between 1 and 50 Cr nm^{-2} have been characterized by different physicochemical techniques and probe reactions of acido-basic properties and of the catalyst oxygen reactivity. They have been tested in oxidative dehydrogenation, ODH of isobutane. The characterization of the catalysts with chemical analysis, XRD, XPS, and Raman spectroscopy has confirmed the general model of the chromium-oxide/alumina catalysts proposed in the literature. The Cr^{6+} species of two types: soluble and insoluble in water have been found at low Cr loading, and Cr_2O_3 in amorphous and crystalline forms have been observed at higher Cr content. The densities of the Cr^{6+} species increase with the increase in the total Cr content to constant values observed at 5–10 Cr nm^{-2} for the water-soluble Cr^{6+} species and at 2 Cr nm^{-2} for the water-insoluble Cr^{6+}. The highest densities of the Cr^{6+} species are 1.6 Cr nm^{-2} and 1.0 Cr nm^{-2} for the water-soluble and insoluble species, respectively. The total initial activity in the ODH of isobutane and the selectivity to isobutene increase markedly with the increase in the Cr loading up to about 10 Cr nm^{-2} and they change only slightly at higher loadings. TOF values referred to the content of Cr^{6+} species (particularly to water soluble Cr^{6+}) do not differ considerably, however, in the wide range of the Cr loading from 2–50 Cr nm^{-2}. This suggests that the dispersed Cr^{6+} species are involved in the active centres of the ODH of IB. Unsupported chromia is more active and less selective (at comparable conversions) than the chromium oxide-alumina catalysts. The differences in catalytic performance between chromia and alumina supported chromium oxide catalysts are ascribed to lower acidity, higher oxygen bond energy, and lower rate of the oxygen chemisorption in the CrAl catalysts, as indicated by isopropanol decomposition probe reaction, oxygen TPD, TPR of hydrogen, and allyl iodide probe reaction.

1. INTRODUCTION

Oxidative dehydrogenation, ODH of isobutane, has attracted some interest in recent years as a route to obtain isobutene, the key reactant for production of methyl tertiary butyl ether (an additive to petrol, replacing the lead-containing compounds) and methacrylates. The classical dehydrogenation (an endothermic reaction) used so far for the production of isobutene has several disadvantages, such as the high reaction temperature, the catalyst deactivation by coke formation, and the consequent need for periodic catalyst regeneration in air. These drawbacks can be avoided in the case of the exothermic oxidative dehydrogenation in the presence of air in the reaction mixture. The catalytic systems reported so far as promising for the ODH of isobutane include the ZnO-TiO_2 system (1), the metal pyrophosphates of which NiP_2O_7 has been found the most active and selective (2), the MgO-V_2O_5 system (3), and Dawson-type heteropolyanions containing tungsten: $K_2P_2W_{17}FeO_6$ (4). The maximum yields of isobutene found for these systems were 8–11% and the selectivities to isobutene at the isobutane total conversion of about 10–20% varied between 50–80%, depending on the system. The reaction temperatures at which they were found active were higher than 400°C. Quite recently we have reported that chromium oxide on different supports is active and selective in the ODH of isobutane already at relatively low temperatures 200–300°C (5, 6). The best catalytic performance has been observed for CrO_x/Al_2O_3, CrO_x/TiO_2 (5), and CrO_x/CeO_2 (6) systems. Chromium oxide supported on lanthanum carbonate has been also found active and selective in this reaction at low temperatures 230–250°C (7).

Supported chromium oxide-based catalysts have been known for many decades as active in many reactions such as polymerization (8), dehydrogenation and dehydrocyclization (9–13) and selective catalytic reduction (SCR) of NO_x with ammonia (14–16). The characterization of these systems has been, hence, a subject of numerous papers (e.g. (17–31) and references therein), aiming at elucidation of active chromium species dispersed on the supports. The chromium-containing catalysts are also active in total oxidation of organic compounds and CO to CO_2 (32). The studies on selective oxidation reactions on supported chromia catalysts are, however, scarce and, beside the preliminary studies on the ODH of isobutane mentioned above (5–7) are limited only to oxidation of methanol on CrO_x/SiO_2

[1] To whom correspondence should be addressed.

0021-9517/98 $25.00

(33,34). The former studies (5) were concerned only with the catalysts of relatively low (1 monolayer, mnl) loading of chromia; no attempt has been made to correlate their catalytic performance in the ODH of isobutane with the catalyst structure and physicochemical properties.

In the present work the alumina supported chromium oxide catalysts of different chromium loading have been characterized by different physico-chemical techniques and tested in the ODH of isobutane. Chemical analysis for the content of oxidized forms of Cr of valency higher than 3+, XPS and Raman spectroscopies, and the TPR technique have been used in an attempt to characterize the nature of the chromium oxide species. Beside these techniques, probe reactions such as isopropanol decomposition (a test of acido-basic properties (35)) and allyl iodide decomposition (a test reaction of the reactivity of the catalyst oxygen (36)) have been performed, in order to determine the overall properties of the catalysts which are considered as essential for activity and selectivity in the hydrocarbon oxidation reactions (37). The chemisorption of oxygen and oxygen TPD have been also studied for some samples. In order to elucidate the modifying action of the alumina support, pure chromia in crystalline and amorphous forms have been examined also, and the results obtained were compared with those for the chromia-alumina catalysts.

2. EXPERIMENTAL

Preparation of the Catalysts

The catalysts were obtained by impregnation with an aqueous solution of chromium nitrate (p.a., POCH, Poland) of the Al_2O_3 support (γ-phase, basic Merck, 111 m^2/g, 60–200 μm), followed by drying for 5 h at 120°C and calcination in a flow of air for 5 h at 500°C. One sample was prepared in an analogous way using chromic acid (CrO_3 p.a. Fluka) as a precursor of the chromia phase. The XPS examination of the pure support did not reveal the presence of K; traces of Na (less than 1 at%) were only observed.

The Cr content varied between ca 1 and 30 at% which corresponded to approximately 0.1–5 theoretical monolayers of Cr_2O_3 on the alumina surface. One monolayer of Cr_2O_3, was estimated from the crystallographic data of the oxide as equivalent to ca 10 at Cr per 1 nm^2 of the support, in agreement with MacIver and Tobin (38). The samples are denoted further in the text by *X* symbols CrAl, where *X* is the number of Cr atoms per square nanometer of alumina support surface.

Amorphous Cr_2O_3 was prepared following the method described by Curry-Hyde and Baiker (39) by slow precipitation from chromium nitrate with ammonia, drying, and treatment at 380°C for 3 h in a stream of hydrogen. Crystalline Cr_2O_3 was obtained by calcination of the amorphous chromia in air at 600°C for 6 h.

Chemical Analysis

The amount of Cr ions in the oxidation state higher than 3+ in the calcined samples was determined with the Bunsen-Rupp (BR) method (40). The method consists in treating a sample with concentrated HCl which leads to reduction of the ions to Cr^{3+} and determination of the chlorine evolved by iodometric titration. At the lowest Cr content the HCl treatment for 30 min dissolved all the chromium introduced in the sample; at higher Cr content a fraction of chromium remains undissolved, even after the prolonged (2 h) treatment in HCl. It should be noted that concentrated HCl does not dissolve the bulk Cr_2O_3. The total amount of chromium dissolved in HCl was determined colometrically as the Cr^{3+} versenate complex.

Following the literature data on the CrO_x/alumina system which shows that Cr^{6+} ions are the main species of valency higher than +3 (13, 19), the total excess charge determined by the BR method was attributed to Cr^{6+} ions only and expressed as a number of Cr^{6+} ions/nm^2 of the catalyst surface, Cr^{6+}_{tot}.

Additionally the amount of Cr^{6+} ions soluble in water (after 1 h treatment at 100°C) was determined colorimetrically as CrO_4^{-2} ($Cr^{6+}_{sol.\,aq.}$). After the treatment with water the amount of oxidized Cr ions remaining in the water-insoluble fraction of the sample, $Cr^{6+}_{ins.\,aq.}$ was analysed with the BR method. Colorimetric determinations were performed using a SPEKOL 32-G315 colorimeter (Carl Zeiss, Jena). The Cr^{3+}-versenate complex was determined at $\gamma = 540$ nm, using a solution of $CrNH_4(SO_4)_2 \cdot 12H_2O$ as a standard. The Cr^{6+} ions were determined as chromates at $\gamma = 400$ nm with $K_2Cr_2O_7$ solution as a standard. The accuracy of the colorimetric analyses was 10 $\mu g \cdot Cr\ ml^{-1}$ which corresponded to 0.05 Cr nm^{-2}.

Specific Surface Area

Specific surface areas of the catalysts, S_{cat}, were determined volumetrically by the BET method, using argon as an adsorbate. The surface area of chromia-coated supports, S^c_{sup} was calculated using the formula: $S^c_{sup} = S_{cat}/(1\text{-}Cr_2O_3$ content per gram of catalyst).

Raman Spectra

These were recorded in ambient conditions with the help of a Dilor XY 800 Raman spectrometer, with the laser radiation source at $\lambda = 514.53$ Å. The range of the spectra varied between 200 and 1100 cm^{-1}.

XRD

XRD diffractograms were recorded with DRON-2 apparatus using CuK_α radiation with a nickel filter. The relative amounts of crystalline Cr_2O_3 in the samples were estimated from the intensity ratio of (116) and (124) diffraction

maxima of Cr_2O_3 and γ-alumina, respectively; the relative integral intensities of the peaks were compared with the calibration curve obtained from the diffractograms of mechanical mixtures of the two oxides. The content of the crystalline Cr_2O_3 in the samples was estimated with an accuracy of $\pm 5\%$.

XPS Measurements

The XPS spectra were recorded with a VG Scientific ESCA-3 spectrometer using Al K$\alpha_{1,2}$ radiation (1486.6 eV) from an X-ray source operating at 12 kV and 20 mA. The working pressure was better than 2×10^{-8} Torr (1 Torr = 133.3 Pa). The binding energies were referenced to the C(1s) peak from the carbon surface deposit at 284.8 eV. Data processing consisted of the calibration of the peak position against the C(1s) line, removal of the background of Shirley's type, and K$\alpha_{3,4}$ peaks, together with routines for the analysis of composite spectra by their fitting with single peaks or doublets. Spectra were decomposed into symmetric gaussian-30%-lorentzian peaks. The relative element content (N_A) was calculated from the formula (41)

$$N = F \cdot I_A \cdot E_A^{0.25} \cdot \sigma_A^{-1} \cdot \exp\left(d_C \cdot \lambda_{C\cdot A}^{-1}\right),$$

where F contains all instrumental factors (including transmission function T) and is assumed to be constant for the measurements, I_A is intensity of the line A measured, E_A is kinetic energy of the A level, σ_A is the elemental cross section for photoionization (42), λ_A is the A-level electrons' inelastic mean free path in the adventitious carbon deposit, and d_C is a thickness of the carbon deposit. The λ and T values were obtained using the Penn approximation (43).

In this study, the Scofield's cross sections were used only for C(1s) ($\sigma_C = 1.0$) and O(1s) ($\sigma_O = 2.93$) lines. In the case of all other XPS and Auger lines, the sensitivity factors were used. They were determined from the element-oxygen intensity ratio in simple oxides, using the "sensitivity" of oxygen equal to its Scofield cross section (2.93) and assuming that the atomic ratio O/Me on the surface of oxides is the same as their stoichiometric ratio. The sensitivity factor of Cr was obtained from a Cr_2O_3 powder treated with hydrogen at 600°C *in situ* in the spectrometer until the O/Cr intensity ratio became constant. The presence of lower valence states of Cr was not detected. The intensity of oxygen was decreased by the content of oxygen bonded with carbon. The value of the Cr sensitivity factor obtained in this way was used in calculations of the content of chromium of all oxidation states. Beside the catalyst samples, also simple compounds: Al_2O_3, Cr_2O_3, and CrO_3 were examined to get the binding energies, BE reference values.

Catalytic Activity Measurements

The activity of the catalysts in the ODH of isobutane was measured in a fixed-bed flow apparatus at 250°C. A stainless steel reactor (120-mm long, ID 13 mm) was coupled directly to a series of gas chromatographs. Isobutene, carbon dioxide, and carbon monoxide were found to be the main reaction products. The amounts of the degradation products (C_2, C_3) and of oxygenates (methacrolein and methacrylic acids) were below 1% of the total amount of products. The carbon balance calculated, taking into account isobutene, CO, and CO_2, was $97 \pm 2\%$ for the conversion of isobutane $\geq 10\%$; at lower conversion the C balance was poorer ($90 \pm 5\%$). The reaction mixture contained 9.2 vol% of isobutane (Phillips Petroleum Corp., 99%) in air.

One half milliliter of catalyst sample (grain size 0.63–1 mm) diluted (1 : 1) with the glass beads of the same diameter were used. It has been checked in the preliminary measurements in which the mass and the grain size of a sample were varied that, under these conditions, the transport phenomena do not limit the reaction rate. For each sample the measurements were performed at contact time between 0.1 and 4 s which was varied by changing the flow rate of the reaction mixture. The total conversion of isobutane did not exceed 20%.

The catalytic data are presented in the form of the plots of selectivities to different products S_p versus the total conversion of isobutane, C. $C = (N_i - N_f)/N_i \times 100$, $S_p = N_p/\sum N_p$, where N_i and N_f are the concentrations of isobutane at the entrance and the exit of the reactor, respectively, and N_p is a concentration of product p in the exit gas. For a given sample the values of C and S were reproducible within 2–5%. The initial total rates of the isobutane disappearance per unit of the catalyst surface, $V^i_{sp\ cat.}$, were also calculated by extrapolating the conversion data to 0 contact time.

A blank test without a catalyst or with glass beads in the reactor showed no conversion of isobutane at the reaction temperature. Pure alumina support was not active either; the isobutane conversion at 250°C was lower than 0.05%. No deactivation of the catalysts was observed during 10 h of the measurement.

Isopropanol Probe Reaction

Decomposition of isopropanol to propene and acetone was studied at 250°C with the pulse method, using dried helium as a carrier gas; 0.1 g of the sample and 2 μl of iPrOH were used and the total flow-rate of helium was 30 ml/min. Analysis of the products was performed by gas chromatography with FID detection. Prior to the measurements the samples were heated at 250°C in dried helium for 2 h. The isopropanol pulses were injected successively until constant values of conversion and amounts of products were attained. The conversion decreased slightly (by 5–10%) with the number of pulses; the propene/acetone ratio remained the same, however. The amounts of products per pulse reported further in the text are the mean of the values obtained in three successive pulses after the stationary state of the activity has been attained. The

pure support was about 10 times less active than the CrAl samples.

Allyl Iodide Probe Reaction

This was studied with the pulse method at 300°C, introducing 2 μl pulses of allyl iodide (Fluka Chemie >97%) into a stream of helium (30 ml/min.); 0.1 g of the samples were used; analysis of the products was performed with gas-chromatography with TCD detection. The main reaction product was CO_2; only traces of acrolein and 1,5 hexadiene were detected. The pulses of allyl iodide were introduced successively until no formation of CO_2 was observed. The samples were pretreated before the measurement for 2 h at 350°C in a stream of dried helium.

TPR Characterization

The experiments were carried out in a gas flow system equipped with a gradientless microreactor (44). The 80% H_2/He mixture was fed to a catalyst sample. In order to minimize the pressure of water evolved during the reduction, which has been found to affect the position of the TPR peaks in the case of some alumina-supported oxides (44,45), 100 mg of a sample were premixed with 1 g of the Al_2O_3 sorbent, precalcinated at 600°C. It has been observed in the preliminary measurements without addition of the alumina, which adsorbs the evolved water, that the TPR peaks were shifted towards the higher temperatures. This effect is the most distinct for unsupported crystalline chromia. The temperature was programmed from 25 to 600°C at 13.3°C/min. The stream leaving the reactor passed through a trap kept at −78°C and the hydrogen consumption was then analysed with a TCD cell. The sample pretreatment before a reduction run consisted of heating in a 6% O_2/He mixture at 500°C for 0.5 h, followed by cooling (0.5 h) in the same mixture to 100°C (0.5 h) and then in pure He to the room temperature. In some experiments the samples were cooled down from 500°C to room temperature in pure He.

TPD of Oxygen

The measurements were carried out in a microreactor coupled to a mass spectrometer VG/Fisons Quartz-200D. About 0.8 g of a catalyst was heated in a stream of dried air at 500° for 2.5 h, cooled down to 200°C in air and then in a stream of dried He to 60°C. The desorption was performed from 60 to 600°C in a stream of He (5 ml/min) at 8°C/min, following the evolution of mass peak $M = 32$.

Chemisorption of Oxygen

This was studied with a gravimetric method using an S 3DV Sartorius microbalance coupled to a conventional vacuum system; 0.5 g of a sample was degassed at 350–375°C at the pressure below 0.13×10^{-3} kPa for 24 h until a constant mass and then cooled down to a measurement temperature. Oxygen (99.0%), purified by vacuum distillation was then introduced and the mass gain was recorded until the constant mass was attained. The measurements were carried out in the temperature range 300–375°C and the oxygen pressure range 0.5–13 kPa. In view of the large volume of the experimental setup the measurements were carried out in isobaric conditions. The accuracy of the measurement was 1 μg. It has been checked in the preliminary experiments that the oxygen uptake was reversible in successive degassing–adsorption cycles.

The control chemical analysis of the 10 CrAl sample after the degassing in vacuum and cooling down to the room temperature has shown a decrease of the total Cr^{6+} content with respect to the fresh sample from about 30% to about 23%. The initial value of the Cr^{6+} content has been, however, restored after the oxygen chemisorption measurements. These facts suggest that the oxygen uptake consists, in fact, in reoxidation of the reduced by vacuum pretreatment Cr^{3+} ions to Cr^{6+}.

3. RESULTS

Basic Characteristics of the Catalysts

Table 1 gives specific surface area, results of chemical analyses for the content of Cr ions of the oxidation state higher than +3 attributed to Cr^{6+}, and the XRD data for the series of CrAl catalysts of different Cr content and for unsupported chromia.

At the lowest Cr content 1 and 2 Cr nm^{-2} the specific surface areas of the catalysts, S_{cat} are higher than that of the alumina support (111 m^2/g) and they decrease with the increase in the Cr loading. The specific surface areas of the chromia-coated support, S^c_{sup} are, with the exception of the 1 CrAl and 2 CrAl samples, practically constant and close to that of the pure support. This indicates that the deposition of the chromium oxide phase does not cause any significant plugging of the alumina pores.

The total amount of the Cr^{6+} ions increases steadily with the increase in the Cr content up to about 5 Cr nm^{-2} and only slightly with the further increase in the Cr loading. The maximum amount of Cr^{6+}_{tot}, 3.3 Cr nm^{-2} is equivalent to about 30% of a monolayer of Cr_2O_3 and 70% of a monolayer of CrO_3 calculated from the crystallographic data of the two oxides. At the lowest Cr loading all chromium is soluble in HCl and is present in the oxidation state 6+. The fraction of Cr soluble in HCl and the fraction of Cr^{6+} ions decrease with the increase in the Cr content and with the appearance of crystalline Cr_2O_3 detected in the XRD analysis.

A part of Cr^{6+} ions is present in the form soluble in water, $Cr^{6+}_{sol.\,aq.}$, and another part in the form of strongly bound, insoluble in water ($Cr^{6+}_{ins.\,aq.}$). The amount of $Cr^{6+}_{sol.\,aq.}$ increases with the increase in the Cr content up to 10 Cr nm^{-2} and remains practically constant at the higher loading; the fraction

TABLE 1

Basic Characteristics of the CrAl Catalysts

Symbol	wt% Cr	S_{cat} m^2/g cat	S_{sup} (calc.) m^2/g	$Cr_{sol.}$ HCl %	Cr^{6+} content Cr^{6+}_{tot}	$Cr^{6+}_{sol.\,aq.}$ at nm^{-2}_{sup}	$Cr^{6+}_{ins.\,aq.}$	XRD analysis' ( )% Cr_2O_3 cryst.
1 CrAl	0.95	127	128	100	0.87	0.32	0.55	γ Al_2O_3
2 CrAl	1.88	122	124	100	1.46	0.47	0.99	γ Al_2O_3
5 CrAl	4.50	111	110	70	2.53	1.51	1.04	γ Al_2O_3
10 CrAl	8.40	104	113	50	2.64	1.70	0.96	γ Al_2O_3
10* CrAl	8.40	110	119	40	2.50	1.70	—	γ Al_2O_3
20 CrAl	15.0	98	115	40	2.52	1.56	1.08	γ Al_2O_3, α Cr_2O_3 (17)
50 CrAl	28.2	82	114	27	2.50	1.77	0.89	γ Al_2O_3, α Cr_2O_3 (25)
Cr_2O_3 cryst.	68.4	28	—	1.3	3.93	3.20	—	α Cr_2O_3
Cr_2O_3 amor.	—	-	-	2.0	0.46	0.25	-	-

* From the chromic acid precursor.

of these species in $Cr^{6+}_{tot.}$ increases with the Cr content from about 40 to 65%. The amount of insoluble species reaches a practically constant value at about 2 Cr nm^{-2}. The values of Cr^{6+}_{tot}, $Cr^{6+}_{sol.\,aq.}$, and $Cr^{6+}_{ins.\,aq.}$ for the samples 10 Cr and 10*Cr prepared respectively from chromium nitrate and chromic acid are practically the same, which suggests that the type of precursor of the chromia phase does not affect the content of the Cr^{6+} ions in the calcined samples. Unsupported chromia show the presence of Cr^{6+} ions on the surface mostly in the form of the water soluble species. The amount of the Cr^{6+} ions is higher for crystalline chromia than for amorphous Cr_2O_3.

The XRD analysis shows the presence of crystalline α-Cr_2O_3 only for the CrAl samples of the highest Cr content: 20 and 50 Cr nm^{-2}. From the relative amounts of Cr_2O_3 phase in the CrAl samples it can be estimated that the fractions of Cr present in the form of crystalline chromia amount to 76% and 61% of total chromium introduced in the samples for samples 20 Cr nm^{-2} and 50 Cr nm^{-2}, respectively. As the fractions of chromium present as hexavalent Cr species are equivalent to 16% and 7.5% of the total amount of Cr, it can be supposed that the remaining chromium (8% and about 30% for catalysts of 20 and 50 Cr nm^{-2}, respectively) is present in the form of amorphous chromia undetected by XRD.

XPS Data

Table 2 summarizes the XPS data for some of the studied samples. The Cr(2p) band was decomposed by fitting the doublet composed of $Cr(2p_{3/2})$ and $Cr(2p_{1/2})$ symmetric peaks as shown in Fig. 1. The band structure was the same as in pure Cr_2O_3. In the case of Cr^{3+} ions also a satellite in the $Cr(2p_{1/2})$ region was taken into account. Under these conditions the experimental spectra were well fitted with two bands above 576 and 579 eV assigned to Cr^{3+} and Cr^{6+} ions, respectively (13, 46–48). The fraction of the Cr^{6+} ions in the total amount of chromium calculated from the relative intensities of the two bands is compared with the results of the BR method, referred to the amount of Cr dissolved in HCl, i.e. to the chromium present in the dispersed state on the surface.

A good agreement between the content of the Cr^{6+} ions estimated by the two methods is observed for catalysts of higher Cr content (10 and 50 CrAl). At lower Cr content the relative amounts of Cr^{6+} ions obtained from the XPS data are lower than those estimated from the chemical analysis. This discrepancy may be due to partial reduction of the samples in the spectrometer owing to the longer the exposition time in the XPS analysis (3–4 h) of the samples of the low Cr loading as compared with 1–2 h for samples 10 and 50 CrAl. The reduction of Cr^{6+} ions in the XPS measurements—a disadvantegous phenomenon in these studies—has been previously observed (48).

TABLE 2

XPS Data for the CrAl Catalysts

Catalyst	BE, eV (FWHM) Cr $2p_{3/2}$ Cr^{3+}	BE, eV (FWHM) Cr $2p_{3/2}$ Cr^{6+}	Cr/Al	%Cr^{6+} XPS	%Cr^{6+} BR
1 CrAl	571.1 (3.5)	580.7 (3.5)	0.04	49	100
2 CrAl	571.1 (3.5)	580.2 (3.5)	0.05	42	81
10 CrAl	577.2 (3.1)	579.8 (3.2)	0.20	56	60.4
10 CrAl[a]	576.9 (3.2)	579.4 (3.3)	0.17	23	4.0
50 CrAl	576.7 (3.3)	579.6 (3.3)	0.37	34	31.5
50 CrAl[a]	576.4 (3.3)	578.8 (3.3)	0.34	18	5.0

[a] After the reaction 10 h at 250°C and cooling in argon.

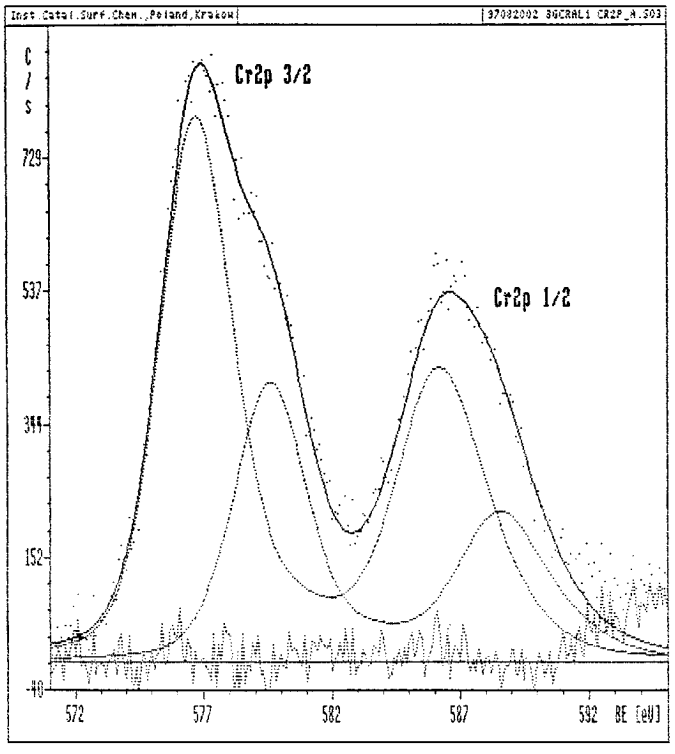

FIG. 1. XPS spectrum of 10 CrAl catalyst in the Cr(2p) region.

The XPS data show also a considerable reduction of the samples after the isobutane reaction. The fractions of Cr^{6+} estimated from the XPS spectra are, however, higher than those obtained by chemical analysis.

The Cr/Al ratio increases with the Cr loading sharply up to ca 10 Cr nm^{-2} and more slowly at higher content. Such behaviour has been previously observed for several oxides systems deposited on supports and explained by agglomeration of the deposited phase with formation of tridimensional crystals at higher loading (49, 50). The dissolution of Cr^{3+} in subsurface layers of γ-Al_2O_3, which would lead to the decrease in the Cr/Al ratio, cannot be excluded either. It should be observed, however, that the formation of a solid solution of Cr^{3+} in Al_2O_3 has been found at temperatures of about 950°C (25), much higher than that used for the preparation of our samples.

The XPS data confirm then the results of XRD, which indicate the formation of Cr_2O_3 at higher Cr concentration. No distinct change in the Cr/Al ratio is observed in the sample after the reaction, which indicates that the Cr dispersion is not modified during the ODH of IB in the studied conditions.

Raman Spectra

Figure 2 shows the Raman spectra for samples 10 CrAl and 10*CrAl. The spectra of both 10CrAl samples show a broad band centered around 840 cm^{-1} with a shoulder around 940 cm^{-1}.

The bands in the 800–1000 cm^{-1} observed under ambient conditions on chromium oxide dispersed on different supports have been ascribed to Cr^{6+} species in the form of chromates of different degrees of oligomerization (23–25). The assignment of the different bands to particular species is difficult in view of the broadness of the spectra. Moreover, the relative intensities of the bands and their positions are different from those reported in the literature. Vuurman *et al.* (25) have observed for the CrO_3/Al_2O_3 catalysts comparable to our chromium content and under the ambient conditions, a large band centered around 896 cm^{-1} with shoulders on both sides at ca 850 and 960 cm^{-1}, and they attributed it to the presence of hydrated dichromate (892 and 362 cm^{-1}) and trichromate species (960 and 850 cm^{-1}). A strong band at 847 cm^{-1} has been reported for monomeric CrO_4^{2-} ion in solution (51), the attribution of our band centered at 840 cm^{-1} to these species seems, however, rather risky in view of the shape of the band. Zaki *et al.* (19) report a small band at 870 cm^{-1} and a broad one centered around 600 cm^{-1} at low content of Cr on Al_2O_3 and the shift of the first band to 900 cm^{-1} with the appearance of a strong, sharp band at 556 cm^{-1} at high Cr loading.

More detailed studies in different conditions are necessary to decide about the exact nature of the chromate

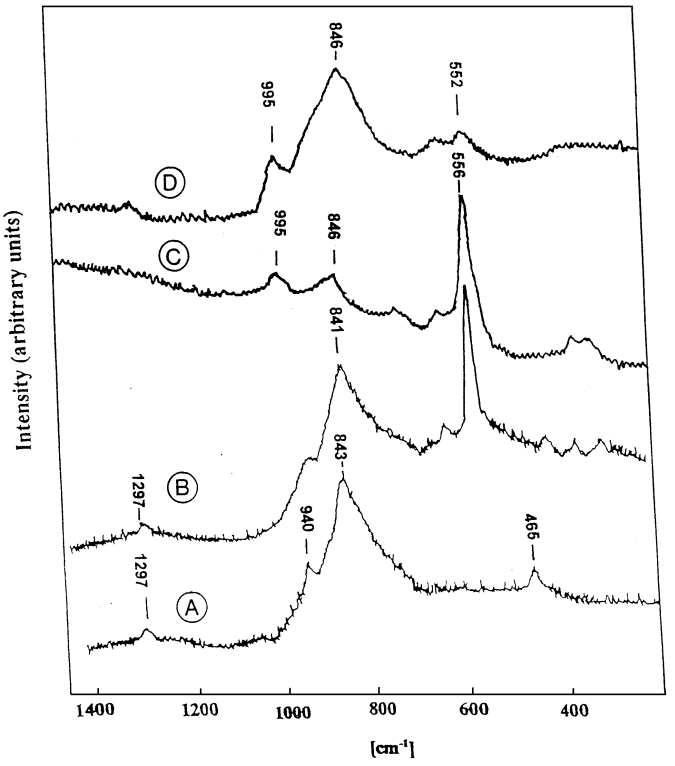

FIG. 2. Raman spectra of 10 CrAl catalysts: A, from chromic acid precursor (10* CrAl); B, from chromium nitrate precursor (10 CrAl); C, after treatment of 10 CrAl sample with water; D, after treatment of 10 CrAl sample with water and recalcination at 350°C.

species in the samples under study. A sharp band at 560 cm^{-1} observed in some spectra can be assigned to crystalline Cr_2O_3 (19, 23). It is clearly seen in the spectrum of the sample 10 CrAl prepared from the chromium nitrate and absent in that prepared from chromic acid.

As seen from Fig. 2 (spectrum C) washing the sample with water and drying leads to considerable decrease in the intensity of the bands in the region 800–1000 cm^{-1}, whereas the band at 550 cm^{-1}, characteristic of Cr_2O_3, persists. After recalcination of the water-washed sample at 350°C the bands characteristic of the chromates are again visible, whereas the intensity of the band at 560 cm^{-1} decreases considerably. This behaviour confirms the removal of a part of hexavalent species on treating with water observed by the chemical analysis and indicates lability of Cr_2O_3 in contact with the alumina support; on heating at relatively mild conditions (350°C) in air this oxide is spread easily, forming the Cr^{6+} species.

Catalytic Activity

Figure 3 presents the dependence of the selectivity to different reaction products on the isobutane conversion at 250°C for catalysts 10 CrAl prepared by impregnation from chromium nitrate and chromic acid and for crystalline Cr_2O_3. The data for the 10 CrAl sample after washing with

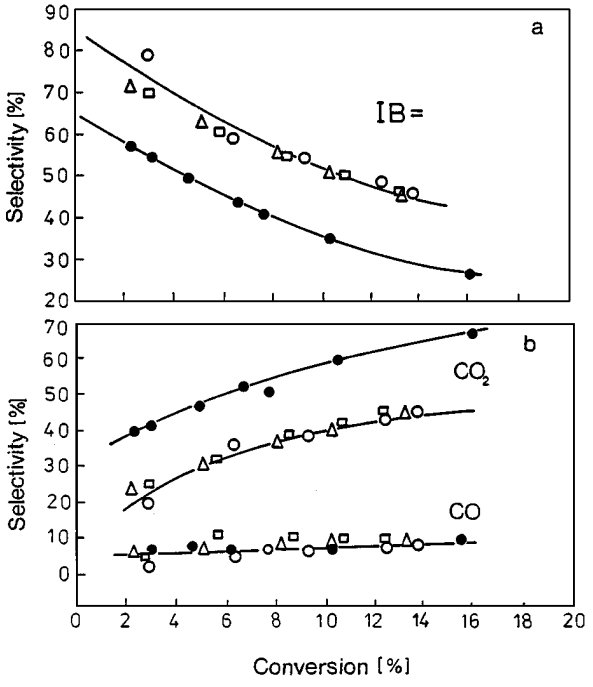

FIG. 3. Selectivity to products of the oxidative dehydrogenation of isobutane for 10 CrAl catalysts and for crystalline chromia as a function of the total isobutane conversion. Reaction temperature: 250°C: Δ, from chromium nitrate precursor (10 CrAl); o, from chromic acid precursor (10* CrAl); □, 10 CrAl catalyst after treatment with water and recalcination at 350°C; ●, crystalline Cr_2O_3.

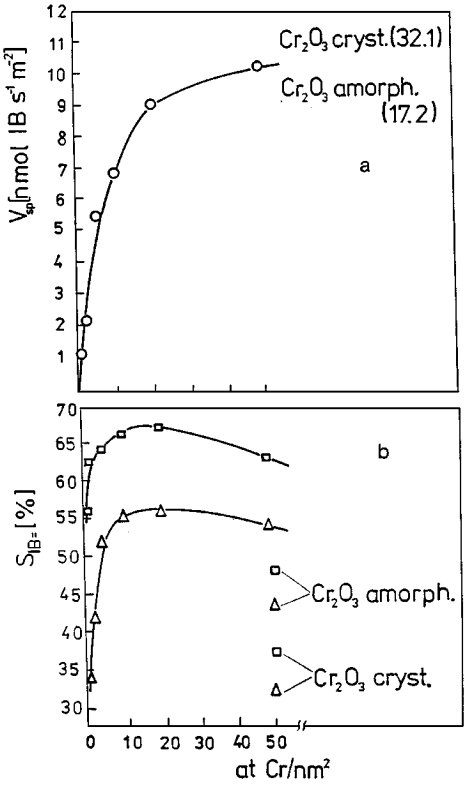

FIG. 4. Dependence of the initial specific activity (a) and of the selectivity to isobutene (b) on the Cr loading for CrO_x/Al_2O_3 catalysts: □, at 5% isobutane conversion; Δ, at 10% isobutane conversion.

water and recalcination at 350°C are also given (squares in Fig. 3). Curves of a similar type have been found for other catalysts. As seen, the selectivity to isobutene decreases as the conversion increases, whereas that to CO_2 increases. This indicates a sequential reaction pathway, in which isobutene formed in the first step is further oxidized to CO_2. The selectivity to CO does not change with the conversion and is lower than that to CO_2. Extrapolation of the curves to the 0 isobutane conversion indicates, moreover, that a fraction of carbon oxides are formed in a parallel route. This fraction is higher for Cr_2O_3 than for the CrAl samples. The results shown in Fig. 3 indicate also that the type of precursor of the chromia phase does not influence the catalytic behaviour. Washing the catalyst with water and recalcination at 350°C does not change the catalytic behaviour, the points corresponding to such treated sample being located on the same selectivity-conversion curve as those for the unwashed catalyst.

In Fig. 4 the variations of the initial specific activity, $V^i_{sp\ cat}$, and the selectivity to isobutene at the isobutane conversions of 5 and 10% at 250°C are plotted as a function of the Cr content. The data obtained for pure chromia, in amorphous and crystalline states are also given. As seen, the specific activity, $V^i_{sp\ cat}$ increases sharply with the increase in the Cr content up to about 10 Cr nm^{-2} and levels off at

TABLE 3

TOF Values for the Isobutane ODH on CrAl, Catalysts at 250°C

Catalyst	TOF × 10^3, isobutane molec. [at (Cr^{6+}) s]$^{-1}$	
	$Cr^{6+}_{tot.}$	$Cr^{6+}_{sol.}$
1 CrAl	0.66	1.79
2 CrAl	0.82	2.56
5 CrAl	1.32	2.25
10 CrAl	1.43	2.24
20 CrAl	1.88	3.03
50 CrAl	1.80	2.55
Cr_2O_3 cryst.	4.92	6.04

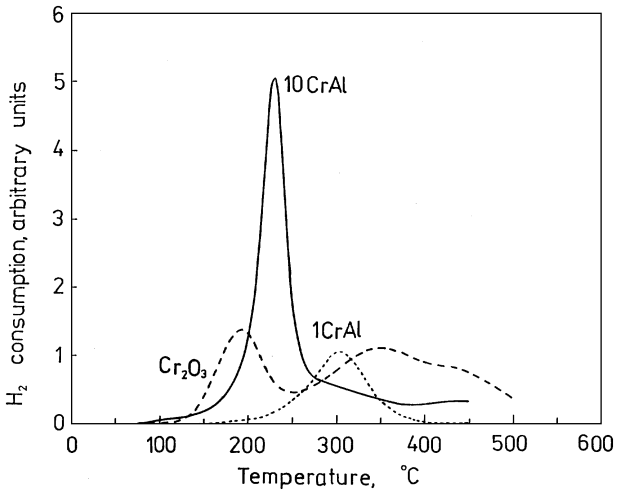

FIG. 5. Hydrogen TPR curves for CrO_x/Al_2O_3 catalysts and for crystalline chromia.

higher Cr loading. The TOF values (Table 3) referring to the content of the Cr^{6+} species do not differ significantly, however, in the whole series of the CrAl catalysts. The TOFs referring to the concentration of Cr^{6+}_{sol} species are practically constant in the Cr loading range from 2–50 Cr nm^{-2}. Those calculated from the total content of Cr^{6+} ions increase with the Cr loading up to about 20 Cr nm^{-2}. Cr_2O_3, both crystalline and amorphous, shows higher activity and higher values of TOF than the most active CrAl samples. The selectivity to isobutene increases up to the Cr content 10–20 Cr nm^{-2} and slightly decreases at higher loading. The maximum values of the isobutene selectivity are higher than those found in the preliminary studies (5) in which different Al_2O_3 was used. Pure chromia is less selective than the mixed CrAl catalysts; lower selectivity is exhibited by crystalline Cr_2O_3, compared with the amorphous sample.

Isopropanol Decomposition

Table 4 gives the rates of formation of propene and acetone in isopropanol decomposition at 250°C on the CrAl catalysts and on chromia samples. Dehydrogenation of isopropanol to acetone is a predominant reaction on the study's samples. The rate of the acetone formation increases with the increase in the Cr content up to ca 10 Cr nm^{-2} and then slightly decreases. The rate of isopropanol dehydration to propene increases up to 5 Cr nm^{-2} and at higher Cr content is practically independent of the Cr content. Crystalline Cr_2O_3 is more active in both dehydrogenation and dehydration reactions. It should be, however, observed that the acetone/propene ratio for crystalline chromia is lower, compared with the CrAl samples.

TABLE 4

Isopropanol Decomposition over CrAl Catalysts, $T = 250$°C

Catalyst	C_3H_6	Acetone	Acetone/C_3H_6
	μmol m^{-2} s^{-1}		
1 CrAl	0.04	0.17	4.3
2 CrAl	0.06	0.29	4.8
5 CrAl	0.10	0.48	4.8
10 CrAl	0.08	0.50	6.3
20 CrAl	0.10	0.45	4.5
50 CrAl	0.10	0.37	3.7
Cr_2O_3 cryst.	0.56	1.33	2.3
Al_2O_3	0.02	0.03	

TPR Results

The TPR curves for some of the CrAl samples and for crystalline chromia are given in Fig. 5. Pure chromia shows a peak around 190°C and additional broad peaks at higher temperatures with maxima around 350 and 450°C. For the CrAl catalysts the first peak, (denoted further in the text as A) is shifted towards higher temperatures, the T_{max} increasing as the Cr loading decreases. These results suggest that the oxygen is more strongly bound in the CrAl catalysts than in unsupported crystalline chromia, the sample of the lowest Cr content 1 Cr nm^{-2} exhibiting the highest oxygen bond energy. Only small consumption of hydrogen at higher temperatures than 300°C is observed for the CrAl samples. The sample of the lowest Cr content, 1 CrAl exhibits only one reduction maximum at about 310°C, and no H_2 consumption at higher temperatures. Curry-Hyde *et al.* (38) have observed for crystalline chromia a main peak at 250°C with a shoulder at 180°C and the weak one at about 360°C. The difference between the position of the low temperature peak in the present studies and those of (38) can be due to different reduction conditions (higher H_2 partial pressure and lower pressure of water vapour in our studies).

For the chromia-alumina catalysts Grunert *et al.* (52) report the main reduction peak at approximately 400°C, no peak being observed by them at lower temperatures. It

TABLE 5

Hydrogen TPR Data for Chromium Oxide-Alumina Catalysts and for Cr_2O_3

Samples	H_2 consumption					
	A			B		
	μmol/g	μmol/m^2	μmol/m$^{2\,a}$	μmol/g	μmol/m^2	H/Cr$_{tot}$
1 CrAl	218.7	1.72	2.17	0	—	2.39
10 CrAl	714.6	6.87	6.17	89.5	0.86	0.88
	660.0[b]	6.34[b]	—	87.5[b]	0.84[b]	
50 CrAl	626.2	7.63	7.40	177.3	2.16	0.23
Cr_2O_3 cryst.	248.5	8.87	9.70	430.6	15.4	0.035
	190.0[b]	6.78[b]	—	420.0[b]	15.0[b]	

[a] Calculated assuming the reduction $Cr^{6+} \rightarrow Cr^{3+} + 0.75\ O_2$.
[b] After cooling down in He.

should be observed, however, that in the latter studies much lower concentration of H_2 (5% in N_2) and the higher rate of the temperature rise (30°/min) were used, compared to our studies.

Table 5 gives the amount of hydrogen consumed in the first peak, A, and the sum of the hydrogen consumption at higher temperatures, B. Column 4 shows the consumption of hydrogen calculated, taking into account the total Cr^{6+} content in the samples obtained from the chemical analysis and assuming that the reduction proceeds according to the stoichiometry $Cr^{6+} \rightarrow Cr^{3+} + 0.75\ O_2$. A good agreement between the experimental and calculated values suggests that the first peak corresponds to the reduction of hexavalent Cr species to Cr^{3+}, according to the formal reaction: $2CrO_3 + 3H_2 \rightarrow Cr_2O_3 + 3H_2O$.

The sample pretreatment in pure He of the 10 CrAl sample changes the hydrogen consumption in peak A by about 7%, which is within the limits of the experimental error. On the other hand, for pure chromia the hydrogen consumption after cooling in He is lower by about 20%, which indicates a higher lability of oxygen in this oxide, compared with the mixed CrAl samples. The He pretreatment does not affect, however, the hydrogen consumption at temperatures higher than about 300°C, B, nor the position of all peaks.

The labile oxygen density in pure chromia, estimated from the reduction data of peak A amounts to 6.0 O At nm^{-2}. This value compares well with the values reported by Kobayashi and Kobayashi (53) and Kobayashi *et al.* (54) for preoxidized Cr_2O_3 (7.4 and 8.6 O At nm^{-2}), obtained with the hydrazine solution method and transient response method, and the data of Miyamoto *et al.* (55) (4.3 and 6.6 O At nm^{-2}), estimated from the reaction of the labile oxygen with rectangular pulses of ammonia. This value is at the same time higher than that reported by Curry-Hyde *et al.* (39) (1.3 O at nm^{-2}). They have ascribed much lower density of oxygen in their TPR studies, compared with the results of Kobayashi *et al.* (53,54) and of Miyamoto *et al.* (55) to the sample pretreatment in Ar, which could remove some of the labile oxygen. As mentioned above the effect of the atmosphere of the sample pretreatment for unsupported chromia has been observed, indeed, in the present studies; the extent of the effect has been found, however, to be rather small.

The hydrogen consumption at higher temperatures (forms B) observed mainly for pure Cr_2O_3 can be due to bulk reduction to lower than 3+ oxidation states, or even to activated hydrogen adsorption reported by Voltz and Weller (56).

The ratio H/Cr$_{tot}$ given in the last column of Table 5 is in good agreement with the data of Niiyama *et al.* (57) obtained for chromia-alumina catalysts of different Cr loading in static reduction studies.

Allyl Iodide Reaction

Figure 6 shows the changes with the number the iodide pulses in the amount of CO_2, formed in the reaction of allyl iodide with the catalyst oxygen for selected samples of the CrAl catalysts and for crystalline Cr_2O_3. The total amount of CO_2 obtained in successive pulses and corresponding to it the amount of the catalyst oxygen which reacted with the allyl species are given in Table 6. As seen the amounts of active oxygen are lower for the CrAl samples, compared with Cr_2O_3. For the CrAl samples they are lower for the catalyst of the lowest Cr loading, 1 Cr nm^{-2}, compared with the 10 CrAl preparations. Also it can be observed that the type of precursor of the chromia phase does not affect significantly the reactivity of oxygen in the calcined catalysts. The difference in the amount of oxygen extricable from the CrAl catalysts and from Cr_2O_3 may be due to the higher density of the reactive oxygen species or/and their lower bonding energy in Cr_2O_3.

The amount of labile oxygen extracted by allyl species from the samples of both CrAl catalysts and Cr_2O_3 is lower than that found in the hydrogen TPR measurements. It

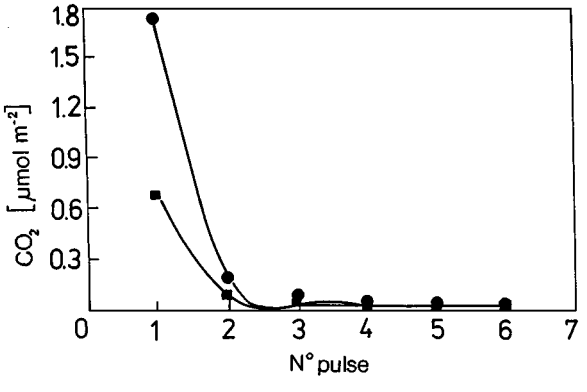

FIG. 6. Change of the amount of CO_2 with the number of pulses of allyl iodide for 10 CrAl catalyst (■), and for crystalline Cr_2O_3 (●).

TABLE 6

Amounts of the Catalyst Oxygen Extracted by Allyl Species for CrAl Catalysts and Cr_2O_3

Catalyst	CO_2 μmol m^{-2}	O at. nm^{-2}	% of active oxygen[a]
1 Cr	0.16	0.20	15
10 CrAl	0.78	0.94	23
10* CrAl	0.66	0.79	21
Cr_2O_3	2.04	2.45	41

* Prepared from chromic acid.

[a] Calculated assuming the reaction $2CrO_3 \rightarrow Cr_2O_3 + 1.5O_2$.

constitutes 15–41% of the active oxygen calculated, taking into account the total content of the Cr^{6+} species and assuming the reaction 2 $CrO_3 \rightarrow Cr_2O_3 + 1.5\ O_2$, whereas in the H_2 reduction practically all the active oxygen can be extracted.

The lower values estimated from the allyl iodide reaction may be due to different exigencies of the organic, large allyl species formed in the allyl iodide decomposition towards the oxygen species, compared with a hydrogen molecule; one may speculate that the allyl species require a special arrangement of the oxygen atoms to react.

TPD of Oxygen

Figure 7 presents the oxygen TPD data for selected CrAl catalysts and for crystalline chromia. A distinct oxygen desorption peak around 400°C and the onset of another desorption process at about 550°C is observed for 10 CrAl catalyst and for Cr_2O_3. It can be observed that the temperature of the onset of the first peak and of the peak maximum for the 10 CrAl catalyst are shifted towards higher temperatures, compared with Cr_2O_3, which suggests higher energy of the oxygen bonding in the mixed sample. No desorption

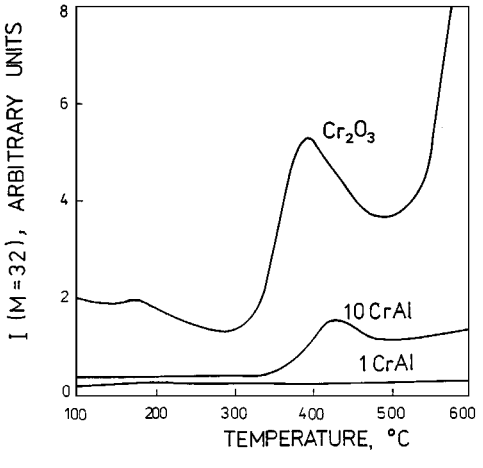

FIG. 7. TPD of oxygen from CrO_x/Al_2O_3 catalysts and unsupported crystalline Cr_2O_3.

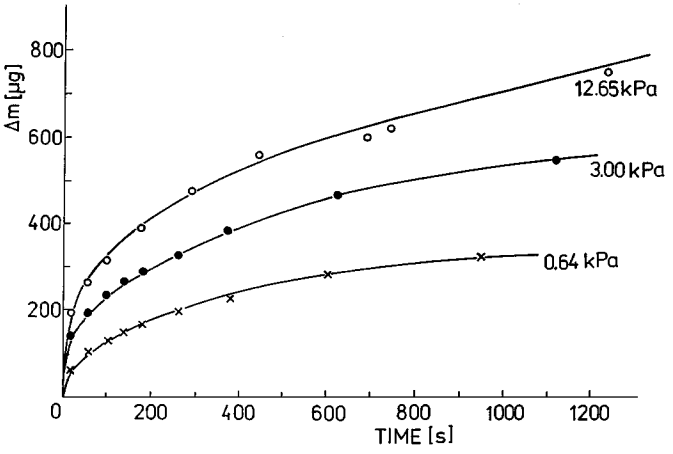

FIG. 8. Kinetics of oxygen uptake at for 350°C 10 CrAl catalyst at different O_2 pressures.

of oxygen up to 600°C has been observed for the sample of the lowest Cr loading 1 Cr nm^{-2}, although the sensitivity of the mass spectrometer assured the detectability of the amount of oxygen contained in the CrO_x species of this catalyst.

Chemisorption of Oxygen

Figure 8 shows changes of the sample mass with the chemisorption time at different oxygen pressures at 350°C for 10 CrAl catalyst. Similar kinetic curves have been observed for amorphous and crystalline samples. The rate of the chemisorption is proportional to $p_O^{0.5}$ which indicates a dissociative adsorption of oxygen. The total mass gain at $t \rightarrow \infty$ at constant temperature and at pressure p, Δm can be then described by a Langmuir adsorption isotherm for a dissociative adsorption,

$$\Delta m = \Delta m_\infty \frac{b p_O^{0.5}}{1 + b p_O^{0.5}},$$

where b is a constant and Δm_∞—a limiting value of Δm for $p \rightarrow \infty$ corresponds to a maximum coverage of a sample with oxygen.

Figure 9 presents the rate of the oxygen uptake at 350°C referred to the value of the initial oxygen pressure $p^{0.5}$ as a function of the oxygen coverage

$$\theta = \Delta m_t / \Delta m_\infty$$

(where Δm_t is a mass gain at time t) for 10 CrAl and Cr_2O_3 in amorphous and crystalline forms.

Table 7 gives the values of the maximum coverage with oxygen and the activation energy values for the rate of the oxygen chemisorption for the three samples. As seen, the maximum oxygen uptake expressed as number of O atoms per square nanometer does not vary significantly for the CrAl sample and for pure chromia. On the other hand, the

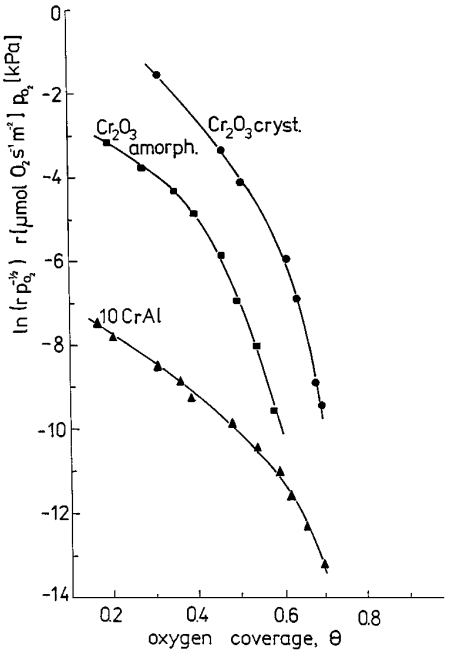

FIG. 9. Rate of the oxygen uptake at 350°C as a function of the oxygen coverage for 10 CrAl catalyst and for crystalline Cr_2O_3.

rates of the oxygen uptake for the three samples are considerably different. The detailed analysis of the kinetics of the oxygen uptake will be a subject of a separate paper (58); at present it can be only observed that the rate of the oxygen chemisorption for 10 CrAl is several orders of magnitude lower, compared with that of crystalline and amorphous chromia, especially at low oxygen coverage. The activation energy of the oxygen chemisorption for pure chromia is at the same time much lower than that of the CrAl sample.

4. DISCUSSION

The data presented above, obtained with chemical analyses, XRD, and Raman spectroscopy are in agreement with the general model proposed previously for the chromium oxide-alumina system (13,19,25). At low Cr loading chromium is present in the form of hexavalent species, a fraction of which is strongly bound to the support surface and another one is easily soluble in water and, thus, interacting only weakly with the alumina. The density of Cr^{6+} increases with the Cr loading to a practically constant value observed at 5–10 Cr nm^{-2} for $Cr^{6+}_{sol.\,aq.}$ and 2 Cr nm^{-2} for $Cr^{6+}_{sol.\,aq.}$ species. The maximum densities of $Cr^{6+}_{sol.\,aq.}$ (1.6 Cr nm^{-2}) and $Cr^{6+}_{ins.\,aq.}$ (1.0 Cr nm^{-2}) compare well with the data of Cavani *et al.* (13), obtained for alumina of lower specific surface area and using chromic oxide as a precursor of the chromium oxide phase. The values calculated from their data are 1.9 and 1.1 Cr nm^{-2} for $Cr^{6+}_{sol.\,aq.}$ and $Cr^{6+}_{ins.\,aq.}$ species, respectively. The total coverage of the alumina surface with Cr^{6+} species amounts to ca 30% of a Cr_2O_3 monolayer and 70% of the CrO_3 monolayer calculated from the crystallographic data of the oxides. Similarly to the data of (13) and (19) at the lowest Cr loading the insoluble Cr^{6+} species predominate over the soluble ones. At higher Cr loading chromia both in amorphous and crystalline forms appear. The XRD data show the presence of crystalline Cr_2O_3 only beginning from 20 Cr nm^{-2}. The Raman spectra and the fact that a considerable fraction of the chromium oxide phase is not soluble in HCl indicate, however, the presence of chromia already in the samples containing 5–10 Cr nm^{-2}. The absence of the Cr_2O_3 pattern in the XRD diffractograms may be due to the low (<3–5 wt%) detectibility limit of the XRD method.

The molecular structure of the hexavalent species on alumina has been a subject of discussion. The Raman spectroscopy and UV-Vis DRS measurements have shown the presence of chromate species of different degrees of polymerization (13, 19, 23–25). Most of the authors agree that at low Cr loading monomeric isolated species are present, where as at higher loadings polymerized forms (dichromates and trichromates) are observed. Cavani *et al.* (13) ascribe the insoluble strongly bound $Cr^{6+}O_x$ species to monomeric groups with T_d symmetry, forming with the support the Cr-O-Al bonds, and the soluble $Cr^{6+}O_x$ to polymeric chromates dispersed over the alumina surface. The data obtained in the present work with Raman spectroscopy show the presence of the chromate species in the catalyst containing 10 Cr nm^{-2}, they do not permit us, however, to determine the degree of their polymerization.

The $Cr^{6+}O_x$ species can be reduced to Cr^{3+} at relatively low temperatures ca 250°C, giving off oxygen. The amount of oxygen which can be extracted depends on the reducing agent. Practically all the $Cr^{6+}O_x$ species can be reduced with hydrogen at 250°C following the reaction $Cr^{6+}O_x \rightarrow Cr^{3+}O_{x-1.5}$, but only about 20% of the active oxygen can be extracted by the allyl intermediate or by the vacuum treatment. The treatment of the samples with deoxygenated helium does not remove the surface oxygen, however, as can be inferred from the TPR data which show practically the same consumption of hydrogen after treatment in oxygen and in helium. Both the absence of the oxygen desorption peak and the shift of the T_{max} in the TPR measurements

TABLE 7

Maximum Coverage with Oxygen, Δm_∞, and Activation Energy, E_a, in Oxygen Chemisorption on CrAl Catalyst and on Pure Cr_2O_3

Catalyst	Δm_∞		E_a	Temperature range
	μmol O_2 m^{-2}	at O nm^{-2}	kJ mol^{-1}	°C
10 CrAl	1.83	1.10	213 ± 10	300–375
Cr_2O_3 cryst.	2.08	1.25	54 ± 5	250–300
Cr_2O_3 amorph.	1.75	1.05	57 ± 5	250–350

for the catalyst of the lowest Cr content, 1 Cr nm^{-2}, indicate, moreover, that the oxygen in the $Cr^{6+}O_x$ species present at this loading (predominantly $Cr^{6+}_{ins.\,aq.}$ groups) is more strongly bound than in the catalysts of the higher Cr loading.

The course of changes of the catalytic activity with the Cr loading indicates that the hexavalent Cr species are involved in active centres of the isobutane reaction on the chromium oxide-alumina catalysts. Partial reduction of the Cr^{6+} species, observed in the catalysts *ex situ* after the reaction, does not permit us to identify them univocally as the active centres; most probably the centre active in the isobutane ODH is composed of a Cr^{6+}/Cr^{3+} redox couple in which the Cr^{3+} ions act as oxygen chemisorption centres. The initial specific activity V^{i}_{sp} increases sharply with the increase in the Cr loading up to about 10 Cr nm^{-2}, i.e. to the saturation coverage of the surface with the $Cr^{6+}O_x$. A small increase in the activity with the further increase in the Cr loading shows that the chromia phase detected at higher Cr content is only a little active. Since the specific activity of unsupported chromia has been found to be quite high, the low activity of Cr_2O_3 present in the CrAl catalysts under study suggests that its specific surface area is very low, compared with that of the species dispersed on alumina. The fact that the catalyst prepared from the chromic oxide precursor, 10* CrAl (in which no Cr_2O_3 was detected by Raman spectroscopy) shows practically the same catalytic performance as the catalyst 10 CrAl in which this oxide was present, also confirms the negligible effect of the chromia phase in the studied catalysts on their activity.

The TOF values referred to total number of Cr^{6+} species, $TOF_{Cr^{6+}_{tot}}$ increase with the increase in the Cr loading up to about 5 Cr nm^{-2} and then only slightly. Practically constant values of TOF referred to the density of the soluble Cr species (2.53 ± 0.14 s^{-1}) are, however, observed in the range 2–50 Cr nm^{-2}. Since at the lowest Cr loading, 1 and 2 Cr nm^{-2}, the insoluble Cr^{6+} species are predominant, the lower $TOF_{Cr^{6+}_{tot}}$ in this range of the Cr content suggest that the insoluble Cr^{6+} species provide active centres of lower activity in the ODH of isobutane than the soluble ones. The lower activity of these species can be related to the higher oxygen bond energy as inferred from the TPR and the oxygen TPD data. The selectivity to isobutene also increases with the Cr loading to a practically constant value, observed at the Cr content corresponding to the saturation coverage of the alumina surface with the dispersed Cr species. The lower selectivity at low Cr coverage can be due to the total combustion of the isobutene on the uncovered surface of the support.

Comparison of the catalytic properties in the ODH of isobutane of the chromium-oxide alumina catalysts with those of unsupported chromia shows that both crystalline and amorphous Cr_2O_3 are more active but less selective (at comparable conversions) to isobutene than the CrAl samples at the optimum range of the Cr loading.

The activity and selectivity in the partial oxidation reactions of hydrocarbons is a complex function of the properties of the catalyst oxygen (including the strength of Me-O bonds in the catalyst, forms of oxygen, and the number of oxygen atoms in the vicinity of the adsorbed hydrocarbon species (37)) and depends also on the acido-basic properties of the catalysts (59). In the ODH of propane and *n*-butane on vanadia-based catalysts the selectivity to olefins has been found to increase with the increase in the oxygen bond energy (60). The increase in the selectivity to olefins with the decrease in the catalyst acidity and the increase in the basicity has been reported for the ODH of propane on titania supported vanadia catalysts promoted with alkali metals (61).

The explanation of the modifying action of the alumina support on the catalytic properties of chromium oxide species can be then sought by comparing the physicochemical properties of the CrAl catalysts with those of unsupported chromia. The allyl iodide test shows that the fraction of the labile oxygen which can be extracted from a solid is higher for unsupported Cr_2O_3 than for the CrAl catalysts. This suggests that oxygen is more strongly bound in the latter case. The shift of the oxygen TPD and hydrogen TPR peaks to higher temperatures for 10 CrAl catalysts, compared with Cr_2O_3 confirms the higher bond energy of the oxygen species in the CrO_x/Al_2O_3. The fact that the hydrogen consumption in the TPR measurements is higher when a Cr_2O_3 sample is pretreated in oxygen than in an inert atmosphere, whereas practically no effect of the pretreatment atmosphere has been observed for the CrAl samples also indicates higher oxygen lability in unsupported Cr_2O_3.

Another factor which can account for the difference in the selectivity to isobutene is the rate of the oxygen uptake, which appears to be equivalent to the reoxidation of the reduced Cr^{3+} species to Cr^{6+}. In the stationary state of the oxidation reactions on oxide catalysts, proceeding by a redox mechanism, the rate of the reoxidation step may determine the coverage of the surface with oxygen (62). The redox mechanism for the ODH reaction has been proposed for the ODH of *n*-butane on vanadia-based catalysts (60). Preliminary studies with the pulse method of the ODH of isobutane on the CrAl catalysts studied in this work have shown practically the same catalytic activity and selectivity in the first pulses with and without gaseous oxygen (63). This suggests that the redox mechanism may operate also in our case. The higher rate of oxygen uptake and lower activation energy of this process for Cr_2O_3, compared with the CrAl catalyst, would suggest then that the coverage of the catalyst surface with oxygen in the stationary state of the isobutane ODH reaction is higher for pure chromia than for the CrAl sample.

In accordance to the general rules for partial oxidation reactions (37) both the higher bond energy of the labile oxygen species and the lower coverage with oxygen

during the catalytic reaction may account for higher selectivity to isobutene in the CrAl catalysts, compared with unsupported chromia.

The difference in the oxygen bond energy in CrO_x species on alumina support and on the unsupported chromia can be due to the interaction of the active phase with the support and the formation of the Cr-O-Al. bonds, which are stronger than those in the Cr-O-Cr chains on Cr_2O_3. The marked difference in the reoxidation rate (the oxygen uptake), on the other hand, suggests that the dissociation of the oxygen molecule and the electron transfer accompanying the passage from O_2 to O^{2-} species are easier for unsupported chromia than for the CrO_x species dispersed on the support. The dissociation of the oxygen molecule requires the presence of the two reduced centers in the vicinity, as has been shown for the V_2O_5-MoO_3 system (64). One may speculate that such an arrangement (the presence of two Cr^{+3} centers in the vicinity) is more probable on unsupported chromia, more easily reduced than the CrO_x species on the CrAl catalysts. Moreover, the electron transfer towards the adsorbed oxygen species should be easier in the case of bulk chromia in which the density of electrons in the bulk should be higher than in the bidimensional, isolated CrO_x groups on alumina.

The higher rate of the propene formation (a measure of the concentration of acidic centres) and the lower acetone/propene ratio (a measure of the basicity (35)) in the isopropanol decomposition, observed for unsupported Cr_2O_3, compared with the CrAl catalysts, suggest higher acidity and lower basicity of Cr_2O_3. The higher selectivity to isobutene observed for the CrAl catalysts could be ascribed then to their lower acidity and higher basicity than those of Cr_2O_3. The higher selectivity to isobutene can be explained, like in the case of the ODH of propane on vanadia-titania catalysts (61, 65), by the easier desorption of isobutene (a base) from the less acidic and more basic surface of the CrAl catalysts, which prevents further reaction of the olefin to carbon oxides. The higher rate of the acetone formation on pure chromia indicates, on the other hand, high concentration of the dehydrogenating centres, which is in keeping with the higher total rate of the reaction on this oxide, compared with chromium oxide-alumina catalysts.

ACKNOWLEDGMENTS

The assistance of Mrs T. Bobińska in preparation and chemical analysis of the catalysts, Mrs Z. Czuła in BET determinations, and Mrs I. Gressel in the isopropanol test is gratefully acknowledged. We also thank Professor Yolande Barbaux of Université d'Artois Lens, France for enabling us with the registration of the Raman spectra. This research was supported by the State Committee for Scientific Research, KBN, under Project No. 3 TO9A 128 09.

REFERENCES

1. Lysova, N. N., Tmenov, D. N., and Luk'yanenko, P., *Russ. Zh. Prikl. Khim*. **65**, 1848 (1992).
2. Takita, Y., Kurosaki, K., Mizuhara, Y., and Tshihara, T., *Chem. Lett.*, 335 (1993).
3. Michalakos, P. M., Kung, M. C., Jahan, I., and Kung, H. H., *J. Catal.* **140**, 226 (1993).
4. Cavani, F., Comuzzi, C., Dolcetti, G., Etienne, E., Finke, R. G., Selleri, G., Trifiro, F., and Trovarelli, A., *J. Catal.* **160**, 317 (1996).
5. Grabowski, R., Grzybowska, B., Słoczyński, J., and Wcisło, K., *Appl. Catal. A* **144**, 335 (1996).
6. Moriceau, P., Grzybowska, B., Barbaux, Y., Wrobel, G., and Hecquet, G., *Appl. Catal. A* **168**, 269 (1998).
7. Hoang, M., Mathews, J. F., and Pratt, K. C., *J. Catal.* **171**, 320 (1997).
8. Mc Daniel, M. P., *Adv. Catal.* **33**, 48 (1985). [Refs. therein]
9. De Rossi, S., Ferraris, G., Fremiotti, S., Indovina, V., and Cimino, A., *Appl. Catal. A: General* **106**, 125 (1993).
10. De Rossi, S., Ferraris, G., Fremiotti, S., Garrone, E., Ghiotti, G., Campa, M. C., and Indovina, V., *J. Catal.* **148**, 36 (1994).
11. Sanfilippo, D., Buonomo, F., Fusco, G., Lupieri, M., and Miracca, I., *Chem. Eng. Sci.* **47**, 2313 (1992).
12. Udomsak, S., and Anthony, R. G., *Ind. Eng. Chem. Res.* **35**, 47 (1996).
13. Cavani, F., Koutyrev, M., Trifirò, F., Bartolini, A., Ghisletti, D., Iezzi, R., Santucci, A., and Del Piero, G., *J. Catal.* **158**, 236 (1996).
14. Kobyliński, T. P., and Taylor, B. W., *J. Catal.* **31**, 450 (1973).
15. Bosch, H., and Janssen, F., *Catal. Today* **2**, 369 (1988).
16. Engweiler, J., Nickl, J., Baiker, A., Köhler, K., Schläpfer, C. W., and von Zelewsky, A., *J. Catal.* **145**, 141 (1994). [Refs. therein]
17. Poole, Jr., Ch. P., and Mac Iver, D. S., *Adv. Catal.* **17**, 224 (1967).
18. Dereń, J., and Haber, J., *in* "Studies on the Physico-Chemical and Surface Properties of Chromium Oxides" (Polish Academy of Sciences-Ceramics Commision, Eds.). Polish Sci., PWN, Kraków, 1969.
19. Zaki, M. I., Fouad, N. E., Leyrev, J., and Knözinger, H., *Appl. Catal.* **21**, 359 (1986).
20. Grünert, W., Shpiro, E. S., Feldhaus, R., Anders, K., Antoshin, G. V., and Minachev, Kh. M., *J. Catal.* **100**, 138 (1986).
21. Cimino, A., Cordischi, D., De Rossi, S., Ferraris, G., Gazzoli, D., Indovina, V., Occhiuzzi, M., and Valigi, M., *J. Catal.* **127**, 761 (1991).
22. Weckhuysen, B. M., Wachs, I. E., and Schoonheydt, A., *in* "Preparation of Catalysts VI" (G. Poncelet, J. Martens, B. Delmon, P. A. Jacobs, and P. Grange, Eds.), Stud. Surf. Sci. Catal. **91**, 151 (1995).
23. Hardcastle, F. D., and Wachs, I. E., *J. Mol. Catal.* **46**, 173 (1988).
24. Vuurman, M. A., Wachs, I. E., Stufkens, D. J., and Oskam, A., *J. Mol. Catal.* **80**, 193 (1993).
25. Vuurman, M. A., Hardcastle, F. D., and Wachs, I. E., *J. Mol. Catal.* **84**, 193 (1993).
26. Schneider, H., Scharf, V., Wokaun, A., and Baiker, A., *J. Catal.* **147**, 545 (1994). [Refs. therein]
27. Weckhuysen, B. M., Schoofs, B., and Schoonheydt, R. A., *J. Chem. Soc., Faraday Trans.* **93**, 2117 (1997).
28. Jóźwiak, W. K., and Dalla Lana, I. G., *J. Chem. Soc., Faraday Trans.* **93**, 2583 (1997).
29. Fountzoula, Ch., Matvalis, H. K., Papadopoulou, Ch., Voyatzis, G. A., and Kofdulis, Ch., *J. Catal.* **172**, 391 (1997).
30. Scierka, S. J., Houalla, M., Proctor, A., and Hercules, D. M., *J. Phys. Chem*. **99**, 1537 (1995).
31. Gazzoli, D., Occhiuzzi, M., Cimino, A., Minelli, G., and Valigi, M., *Surf. Interface Anal.* **18**, 315 (1992).
32. Fouad, N. E., Knözinger, H., and Zaki, M. I., *Z. Phys. Chem*. **203**, 131 (1998).
33. Parlitz, B., Hanke, W., Fricke, R., Richter, M., Roost, V., and Öhlmann, G., *J. Catal.* **94**, 24 (1985).
34. Kim, D. S., Tatibouët, J. M., and Wachs, I. E., *J. Catal.* **136**, 209 (1992).
35. Ai, M., *Bull. Chem. Soc. Jpn*. **49**, 1328 (1976).
36. Grzybowska, B., Janas, J., and Haber, J., *J. Catal.* **49**, 150 (1977).
37. Bielański, A., and Haber, J., "Oxygen in Catalysis," Dekker, New York, 1991. [Refs. therein]
38. Mac Iver, D. S., and Tobin, H. H., *J. Phys. Chem*. **64**, 451 (1960).

39. Curry-Hyde, H. E., and Baiker, A., *Appl. Catal.* **65**, 211 (1990).
40. Dereń, J., Haber, J., and Słoczyński, J., *Chem. Anal.* **6**, 659 (1961). [Polish]
41. Szajman, J., Liesegang, J., Jenkin, J. G., and Leckey, R. C. G., *J. Electron Spectrosc. Relat. Phenom.* **23**, 97 (1981).
42. Scofield, J. H., *J. Electron Spectrosc.* **8**, 129 (1976).
43. Penn, D. R., *J. Electron Spectrosc.* **9**, 29 (1976).
44. Zieliński, J., *J. Catal.* **76**, 157 (1982).
45. Zieliński, J., *Catal. Lett.* **12**, 389 (1992).
46. Grünert, W., Shpiro, E. S., Feldhaus, R., Anders, K., Antoshin, G. V., and Minachev, Kh. M., *J. Catal.* **100**, 138 (1986).
47. Okamoto, Y., Fujii, M., Imanaka, T., and Teramishi, S., *Bull. Chem. Soc. Jpn.* **49**, 859 (1976).
48. Rahman, A., Mohamad, M. H., Ahmed, M., and Aitari, A. M., *Appl. Catal. A* **121**, 203 (1995).
49. Bond, G. C., Zurita, J. P., and Flamerz, S., *Appl. Catal.* **27**, 353 (1986).
50. Mendialdua, J., Barbaux, Y., Gengembre, L., Bonnelle, J. P., Grzybowska, B., and Gąsior, M., *Bull. Pol. Acad. Sci. Chem.* **35**, 213 (1987).
51. Michel, G., and Cahay, R., *J. Raman Spectrosc.* **17**, 4 (1986).
52. Grünert, W., Saffert, W., Feldhaus, R., and Anders, K., *J. Catal.* **99**, 149 (1986).
53. Kobayashi, M., and Kobayashi, H., *Bull. Chem. Soc. Jpn.* **49**, 3009, 3018 (1976).
54. Kobayashi, M., and Kanno, T., *J. Chem. Soc. Faraday Trans. I* **85**, 579 (1989).
55. Miyamoto, A., Ui, T., and Murakami, Y., *J. Catal.* **80**, 106 (1983).
56. Voltz, S. E., and Weller, S. W., *J. Amer. Chem. Soc.* **76**, 4695, 4701 (1954).
57. Niiyama, H., Murata, K., Ebitani, A., and Echigoya, E., *J. Catal.* **48**, 194 (1977).
58. Słoczyński, J., and Kozłowska, A., to be published.
59. Grzybowska-Świerkosz, B., *Mater. Chem. Phys.* **17**, 121 (1987). [Refs. therein]
60. Kung, H. H., *Adv. Catal.* **40**, 1 (1994).
61. Grabowski, R., Grzybowska, B., Samson, K., Słoczyński, J., Stoch, J., and Wcisło, K., *Appl. Catal. A* **125**, 129 (1995).
62. Mars, P., and van Krevelen, D. W., *Chem. Eng. Sci., Sp. Suppl.* **3**, 41 (1954).
63. Grzybowska, B., and Gressel, I., in press.
64. Najbar, M., Wal, W., and Chrząszcz, J., *Stud. Surf. Sci. Catal.* **55**, 779 (1990).
65. Grabowski, R., Grzybowska, B., Kozłowska, A., Słoczyński, J., and Wcisło, K., *Topics Catal.* **3**, 277 (1996).